Cell Reports, Volume *39*

Supplemental information

Cryo-EM structures of SARS-CoV-2 Omicron BA.2 spike

Victoria Stalls, Jared Lindenberger, Sophie M.-C. Gobeil, Rory Henderson, Rob Parks, Maggie Barr, Margaret Deyton, Mitchell Martin, Katarzyna Janowska, Xiao Huang, Aaron May, Micah Speakman, Esther Beaudoin, Bryan Kraft, Xiaozhi Lu, Robert J. Edwards, Amanda Eaton, David C. Montefiori, Wilton B. Williams, Kevin O. Saunders, Kevin Wiehe, Barton F. Haynes, and Priyamvada Acharya

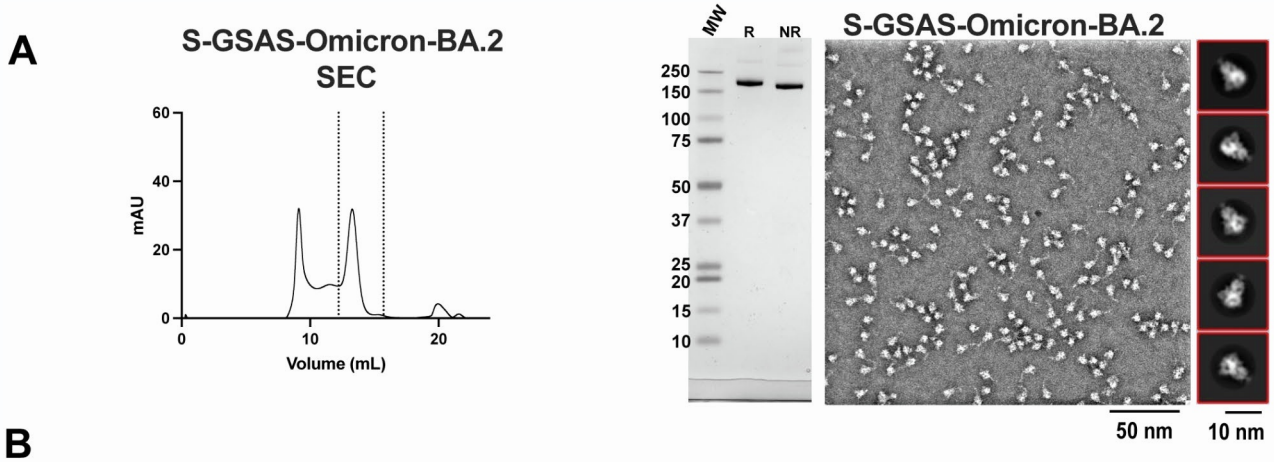

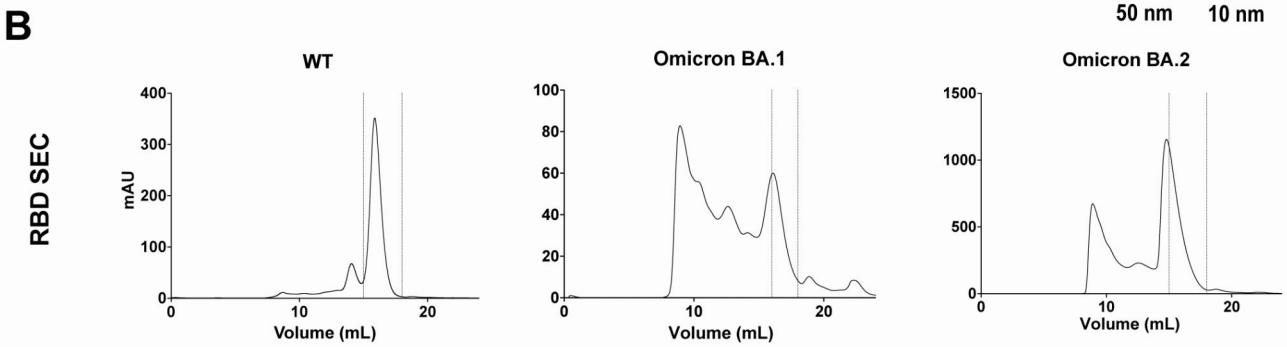

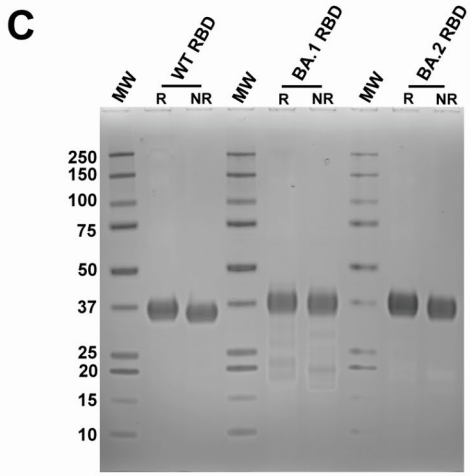

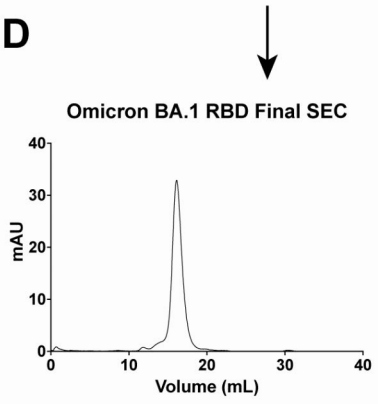

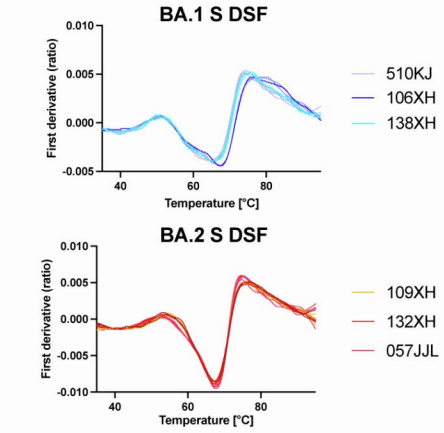

	Lot #	Ti#1 Mean ± St Dev	Ti#2 Mean ± St Dev	Ti#3 Mean ± St Dev
S-GSAS-Omicron-BA.1	510KJ	50.7 ± 0.1	64.9 ± 0.9	74.1 ± 0.3
	106XH	50.8 ± 0.2	67.4 ± 0.2	77.0 ± 0.9
	138XH	50.9 ± 0.9	65.4 ± 0.5	75.2 ± 0.6
S-GSAS-Omicron-BA.2	109XH	54.5 ± 0.4	67.5 ± 0.1	76.0 ± 0.8
	132XH	53.6 ± 0.6	67.4 ± 0.3	76.3 ± 0.5
	057JJL	52.5 ± 1.0	67.6 ± 0.2	74.9 ± 0.3

Figure S1. Quality control of SARS-CoV-2 S proteins and RBD proteins, Related to Figures 1 and 2. (A) S-GSAS-Omicron-BA.2: (left) Size Exclusion Chromatography (SEC) with dashed lines indicating peak fractions pooled for final sample. (middle-left) SDS-PAGE: lane 1 molecular weight marker, lane 2 Reduced (R), and Non-reduced (NR) of 2 µg Spike protein. (middle-right) Representative micrograph with 50 nm scale bar, and (right) 2D class averages with 10 nm scale bar. **(B)** From left to right SEC curves of WT, Omicron-BA.1, and Omicron-BA.2 RBDs, with dashed lines showing pooled fractions. **(C)** RBD protein SDS-PAGE with molecular weight marker, WT R and NR, Omicron-BA.1 R and NR, and Omicron-BA.2 R and NR. **(D)** Second and final SEC of Omicron-BA.1 RBD taken from pooled fractions indicated in B. **(E)** DSF plots of S-GSAS-Omicron BA.1 and BA.2 separated by lots. All lots were ran with three technical replicates, except 057JJL which had 6. Bottom table shows inflection temperatures ± standard deviation. *Fig 2A also includes data from lots 106XH and 109XH.

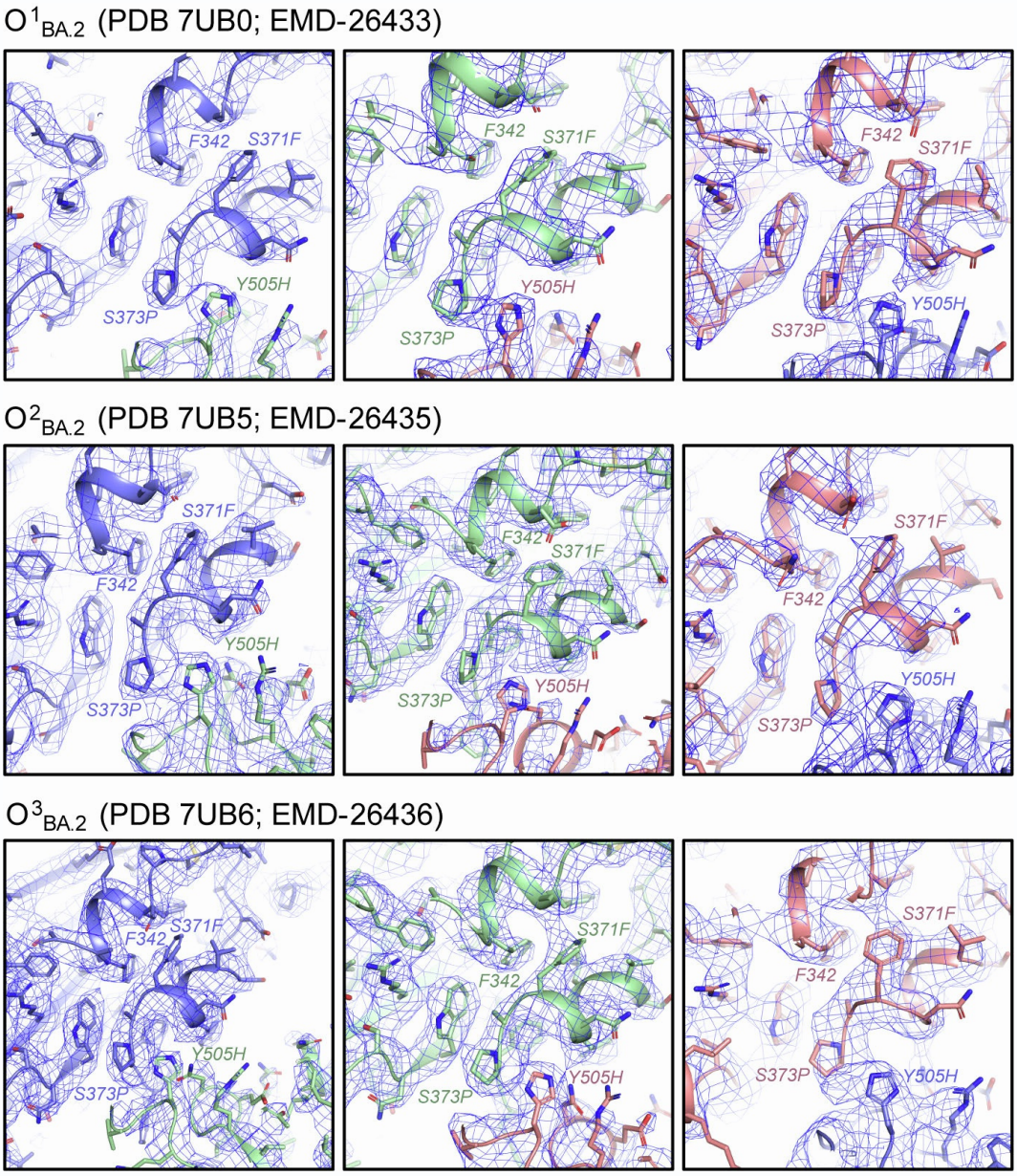

Figure S2. View of RBD interfacial region bearing S371F and S373P substitutions, Related to Figures 1 and 3. Cryo-EM reconstructions are shown as blue mesh with underlying fitted model in cartoon and side chains in sticks. Each panel shows the packing of the RBD region bearing the S371F and S373P substitutions with the RBD helix bearing residue F342, as well as inter-protomer packing with the adjacent RBD Y505H substitution stacking against P373. Details are shown for each protomer in $O^1_{BA.2}$ (top row), $O^2_{BA.2}$ (middle row) and $O^3_{BA.2}$ (bottom row).

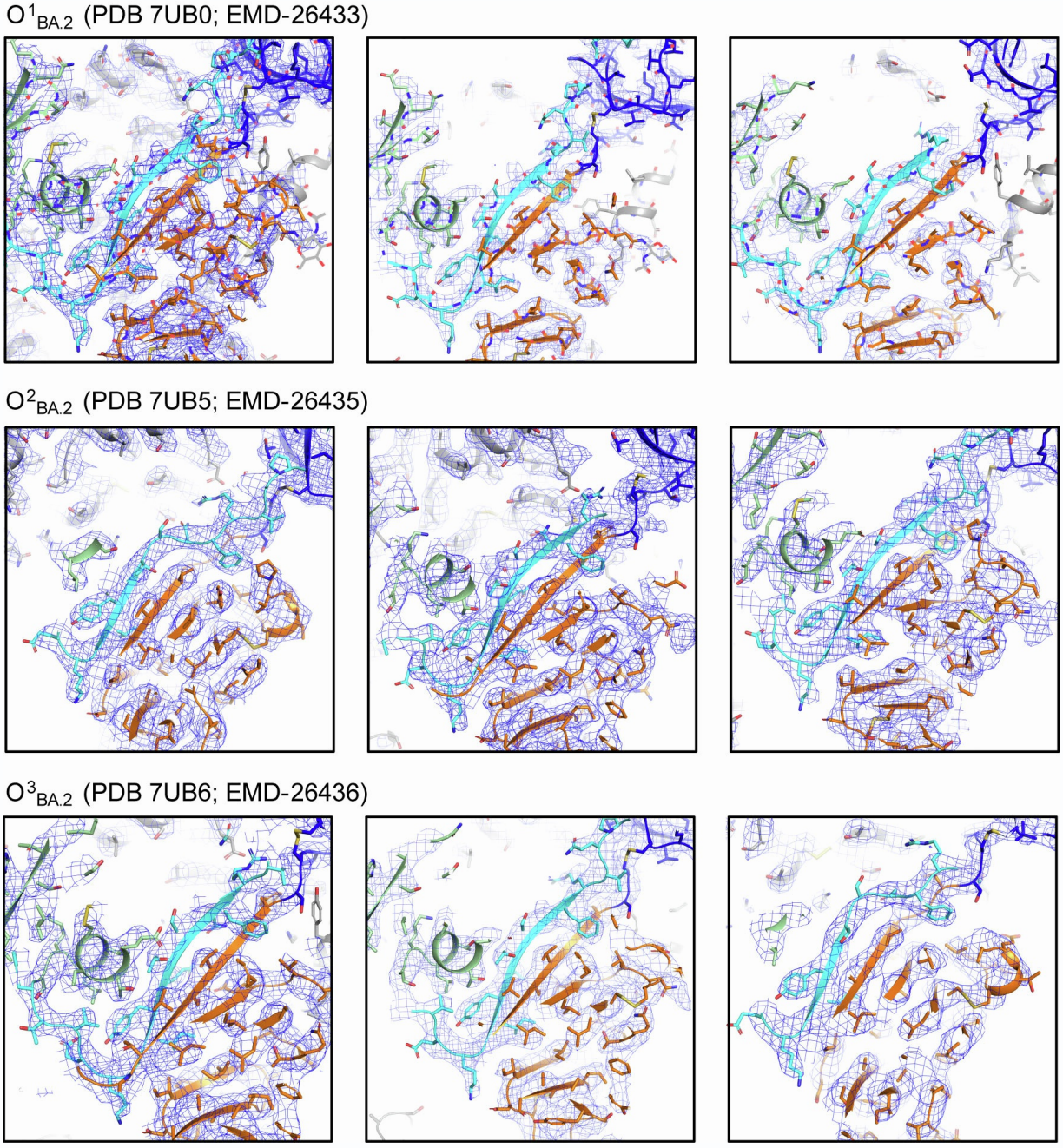

Figure S3. View of NTD-to-RBD (N2R) linker in 3-RBD-down Omicron BA.2 S, Related to Figure 4. Cryo-EM reconstructions are shown as blue mesh with underlying fitted model in cartoon and side chains in sticks. Each panel shows the N2R linker (cyan) of a protomer stacked against its SD2 subdomain (orange). The NTD is colored green and SD1 subdomain blue. Details are shown for each protomer in $O^1_{BA.2}$ (top row), $O^2_{BA.2}$ (middle row) and $O^3_{BA.2}$ (bottom row).

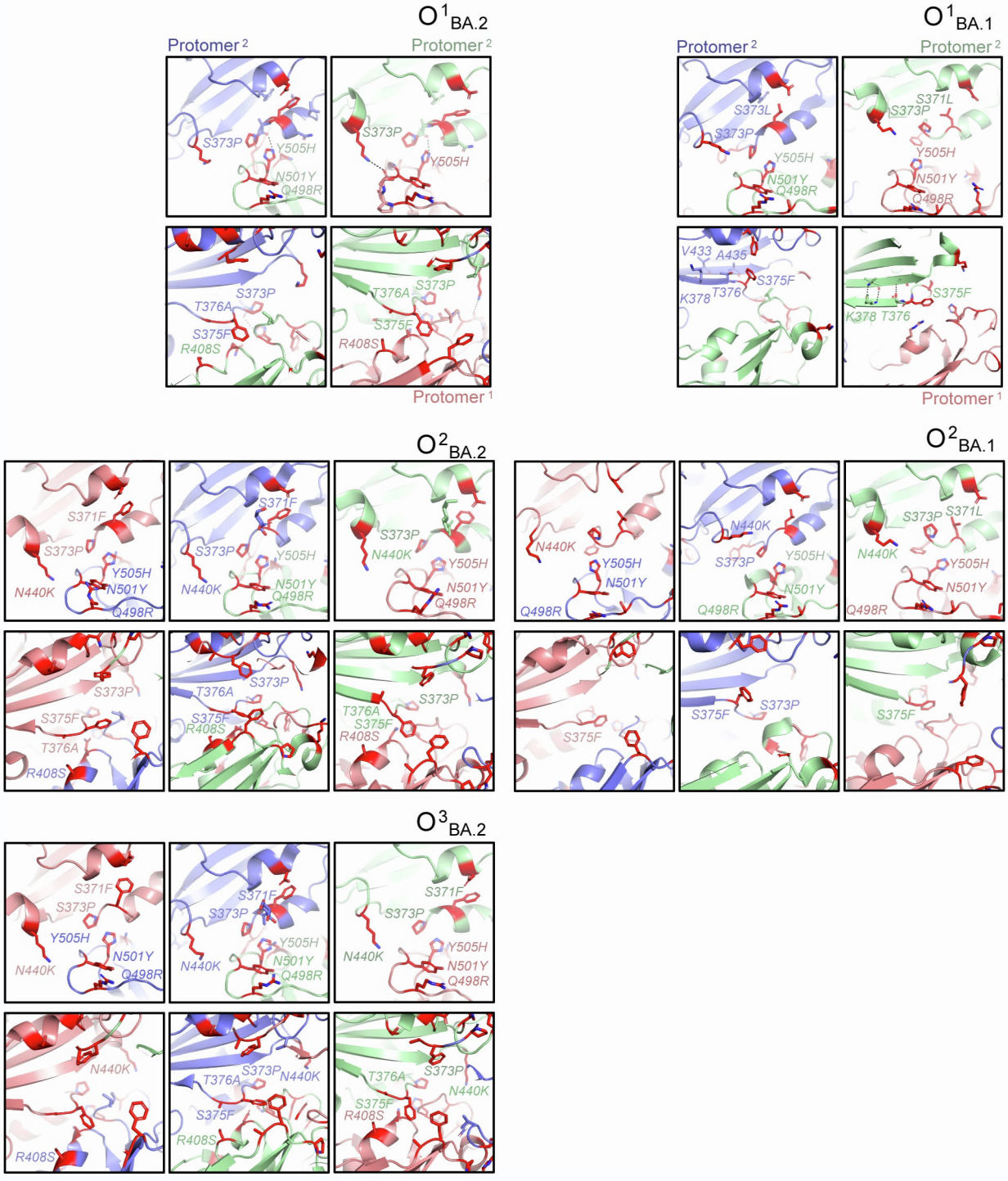

Figure S4. Comparison of the RBD-RBD interface in the Omicron BA.1 and BA.2 S 3-RBD-down structures, Related to Figure 3. Interprotomer interactions between adjacent RBDs are shown for (left) the BA.2 S protein structures ($O^1_{BA.2}$: PDB 7UB0; $O^2_{BA.2}$: PDB 7UB5; $O^3_{BA.2}$: PDB 7UB6), and (right) the BA.1 S protein structures ($O^1_{BA.1}$: PDB 7TF8; $O^2_{BA.1}$: PDB 7TL1)

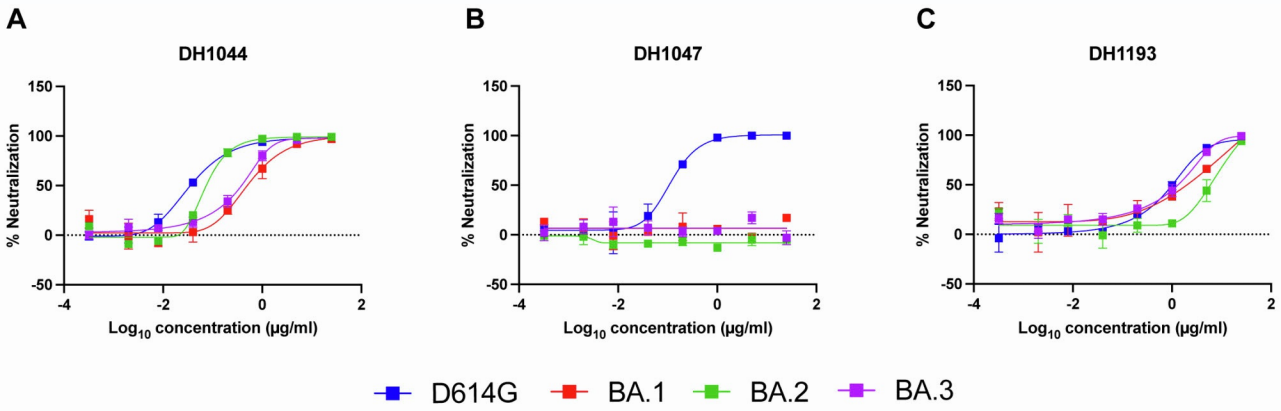

D

	D614G		Omicron -BA.1		Omicron -BA.2		Omicron -BA.3	
	ID50	ID80	ID50	ID80	ID50	ID80	ID50	ID80
DH1044	0.04	0.17	0.52	2.3	0.09	0.19	0.35	0.99
DH1047	0.1	0.34	>25	>25	>25	>25	>25	>25
DH1193	1	3.7	2	11	6.1	16	1.3	4.4

Figure S5. Pseudovirus neutralization by RBD-directed antibodies. Related to Figure 5. A. DH1044, **B.** DH1047, and **C.** DH1193. **D.** ID50 and ID80 values in µg/ml. Neutralization data are presented as the mean of 2 technical replicates within the same assay and the error bars indicate the percent difference between the duplicate wells at each dilution. The neutralization data were log transformed and then fitted with an asymmetric five-parameter curve within Graphpad Prism. The ID50 and ID80 values represent the antibody concentration necessary to achieve 50% and 80% neutralization of each virus tested.

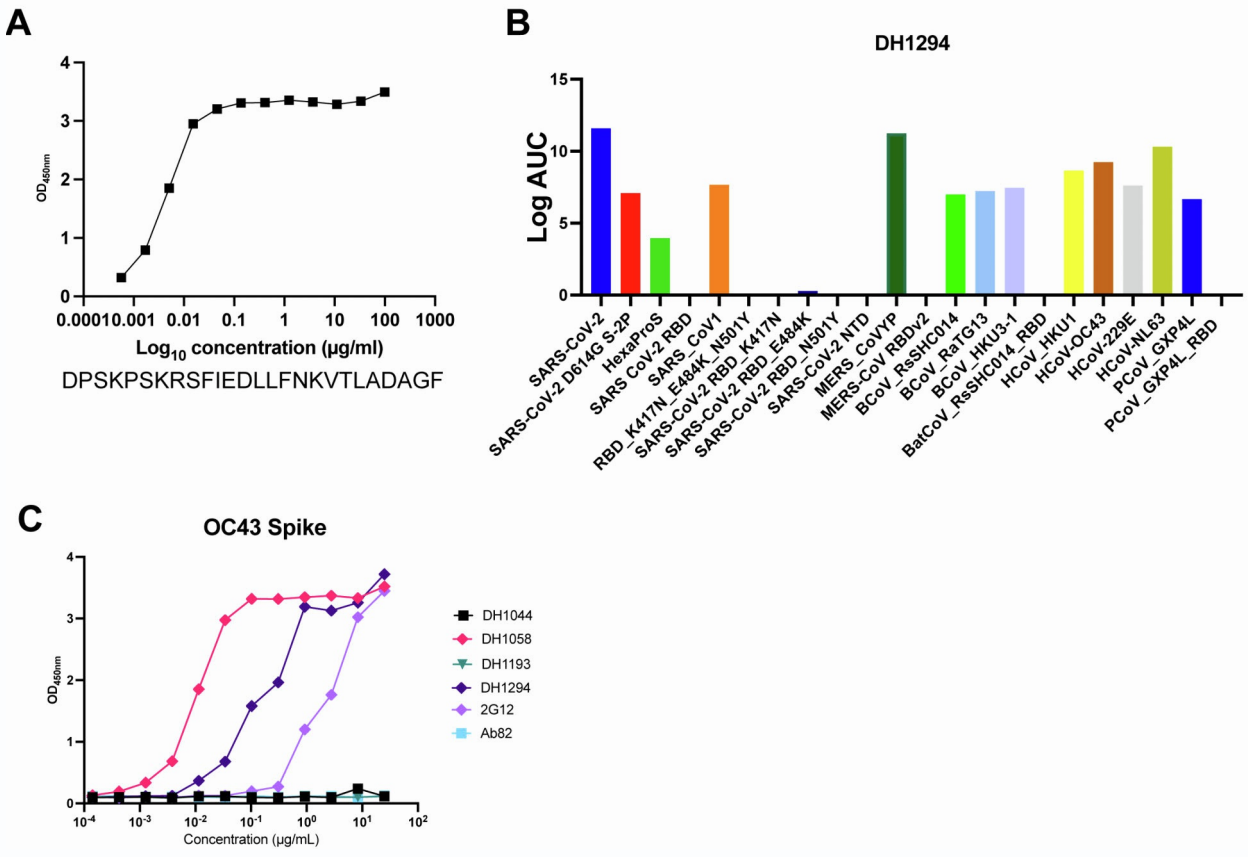

Figure S6. Epitope mapping of fusion peptide directed antibody DH1294, Related to Figure 7. A. Binding of antibody DH1294 to the fusion peptide (sequence indicated below)**. B.** ELISA binding of DH1294 to diverse CoV spikes. **C.** ELISA binding of antibodies to the CoV OC43 spike.

Table S1: Cryo-EM data collection and refinements statistics
S-GSAS-Omicron-BA.2, related to Figures 1, 3, 4, 6, 7, S2-S4, Data S2-S3.

	3-down			1-up		1.5-up
PDB ID	7UB0	7UB5	7UB6	n/a	n/a	n/a
EMDB ID	26433	26435	26436	26644	26647	26643
Data Collection and processing						
Microscope	FEI Titan Krios					
Detector	Gatan K3					
Magnification	81000					
Voltage (kV)	300					
Electron exposure (e-/Å^2)	54.7					
Defocus Range (μm)	2.6 to 0.8					
Pixel size (Å)	1.08					
Reconstruction software	cryoSPARC					
Symmetry imposed	C1	C1	C1	C1	C1	C1
Initial particle images (no.)						
Final particle images (no.)	411,890	276,707	198,211	70,271	114,624	54,450
Map resolution (Å)	3.31	3.35	3.52	3.93	3.74	3.98
FSC threshold	0.143	0.143	0.143	0.143	0.143	0.143
Refinement						
Initial model used	7KDK	7KDK	7KDK			
Model composition						
Nonhydrogen atoms	25,039	24,963	24,762			
Protein residues	3,112	3,107	3,105			
R.M.S. deviations						
Bond lengths (Å)	0.004	0.004	0.004			
Bond angles (°)	0.651	0.663	0.669			
Validation						
MolProbity score	1.22	1.29	1.24			
Clashscore	3.25	2.74	2.96			
Poor rotamers (%)	0	0	0			
EM ringer score	3.44	3.13	2.97			
Ramachandran plot						
Favored regions (%)	97.49	96.47	97.19			
Allowed (%)	2.51	3.53	2.81			
Disallowed regions (%)	0	0	0			

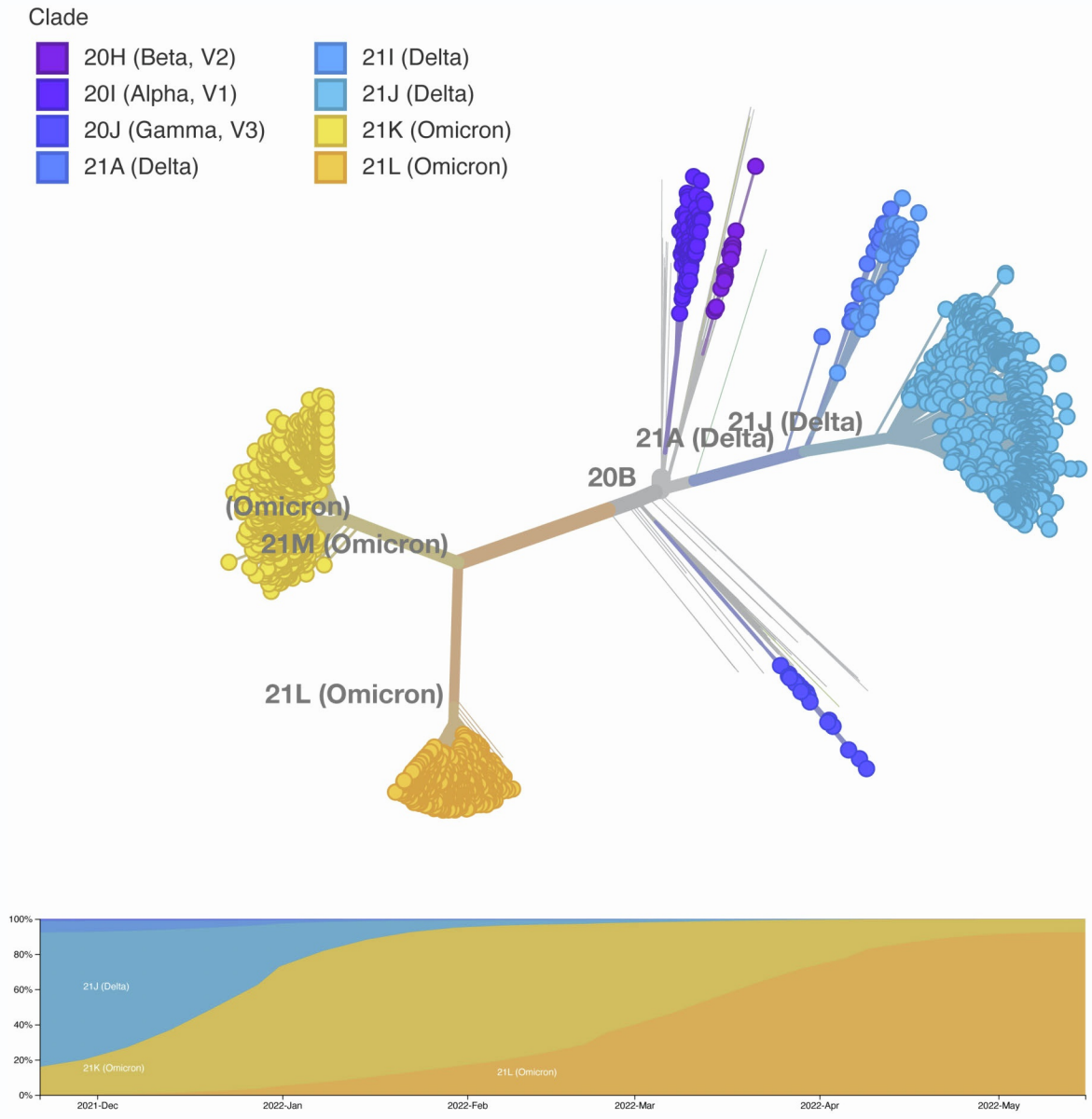

Data S1. Emergence and spread of the SARS-CoV-2 Omicron variant lineages, Related to Figure 1. Top. Phylogenetic tree of SARS-CoV-2 variants of concern. **Botttom.** Global frequencies of SARS-CoV-2 variants plotted against time from April 2021 to May 2022.

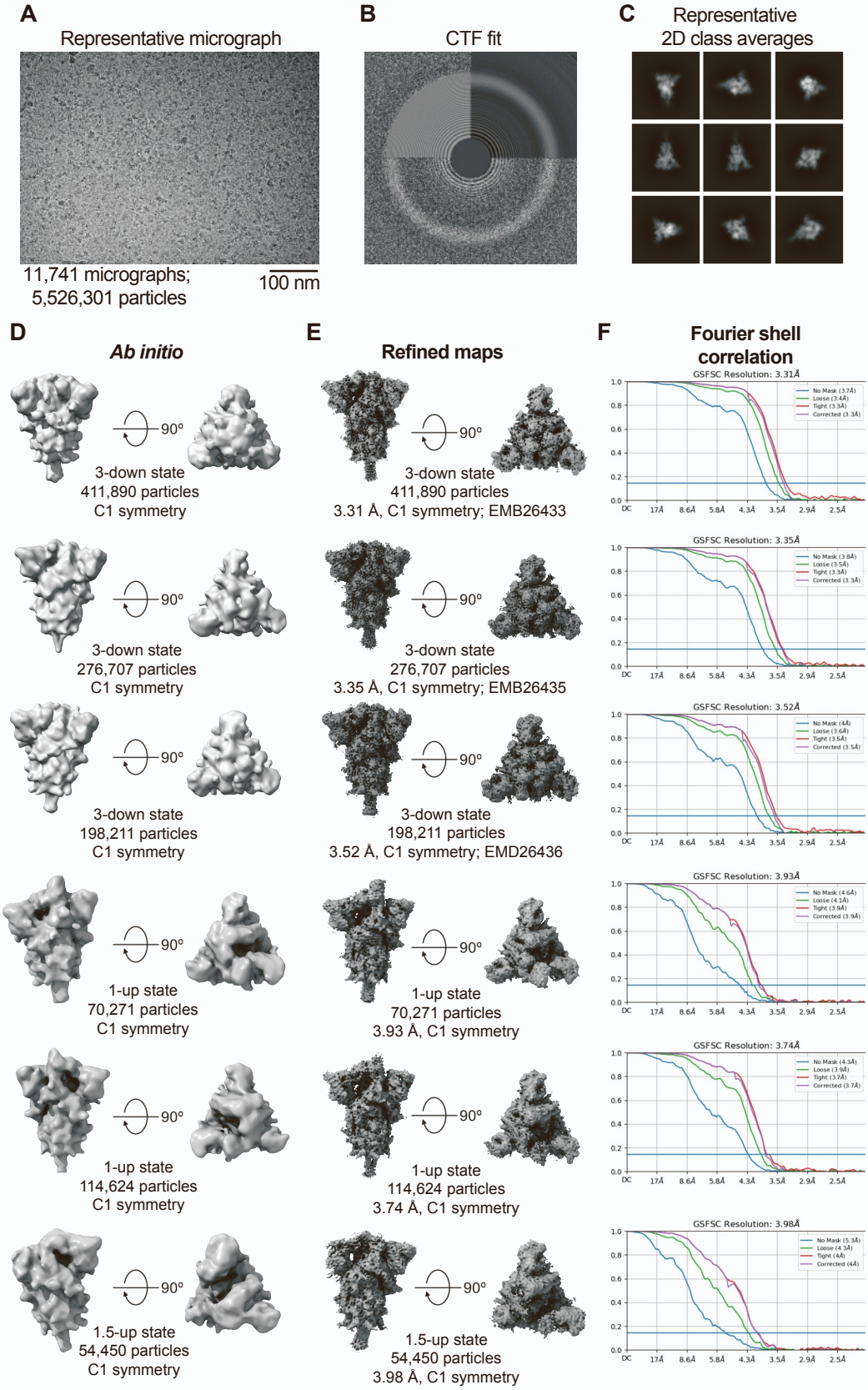

Data S2. Cryo-EM data processing for the S-GSAS-Omicron SARS-CoV-2 S ectodomain, Related to Figure 1, Table S1. (A) Representative micrograph. **(B)** CTF Fit. **(C)** Representative 2D class averages from cryo-EM dataset. Box size = 345.6 Å. **(D)** Ab initio reconstructions for the cryo-EM 3-RBD-down, 1-RBD-up, and 1.5-RBD-up states. **(E)** Refined maps for the cryo-EM corresponding states. **(F)** Fourier shell correlation curves for the cryo-EM corresponding states.

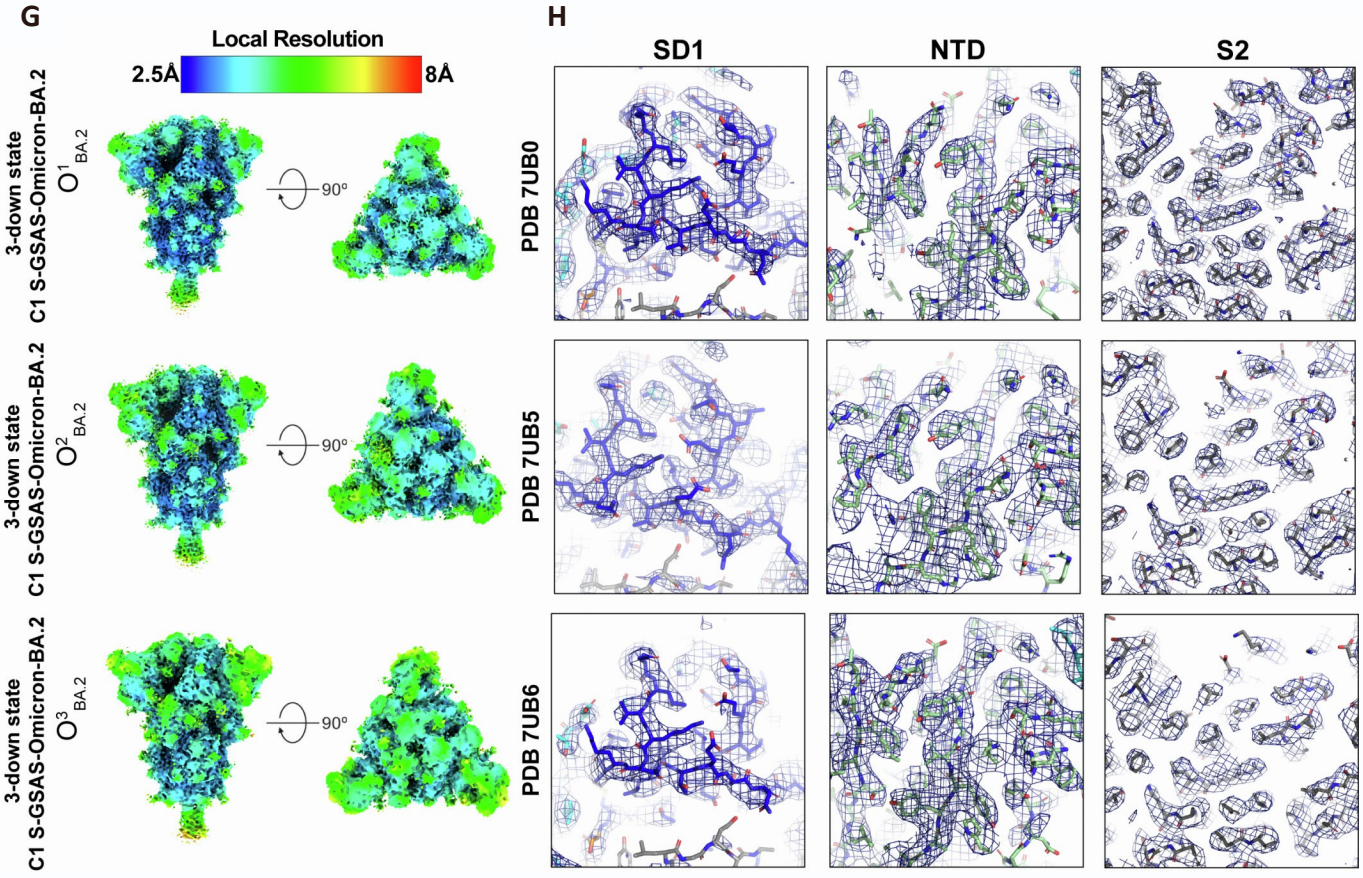

Data S2 continued. Cryo-EM data processing for the S-GSAS-Omicron SARS-CoV-2 S ectodomain, Related to Figure 1, Table S1. (G) Refined maps colored by local resolution ranging from 2.5 Å to 8 Å. **(H)** Zoomed in views of SD1, NTD, and S2.

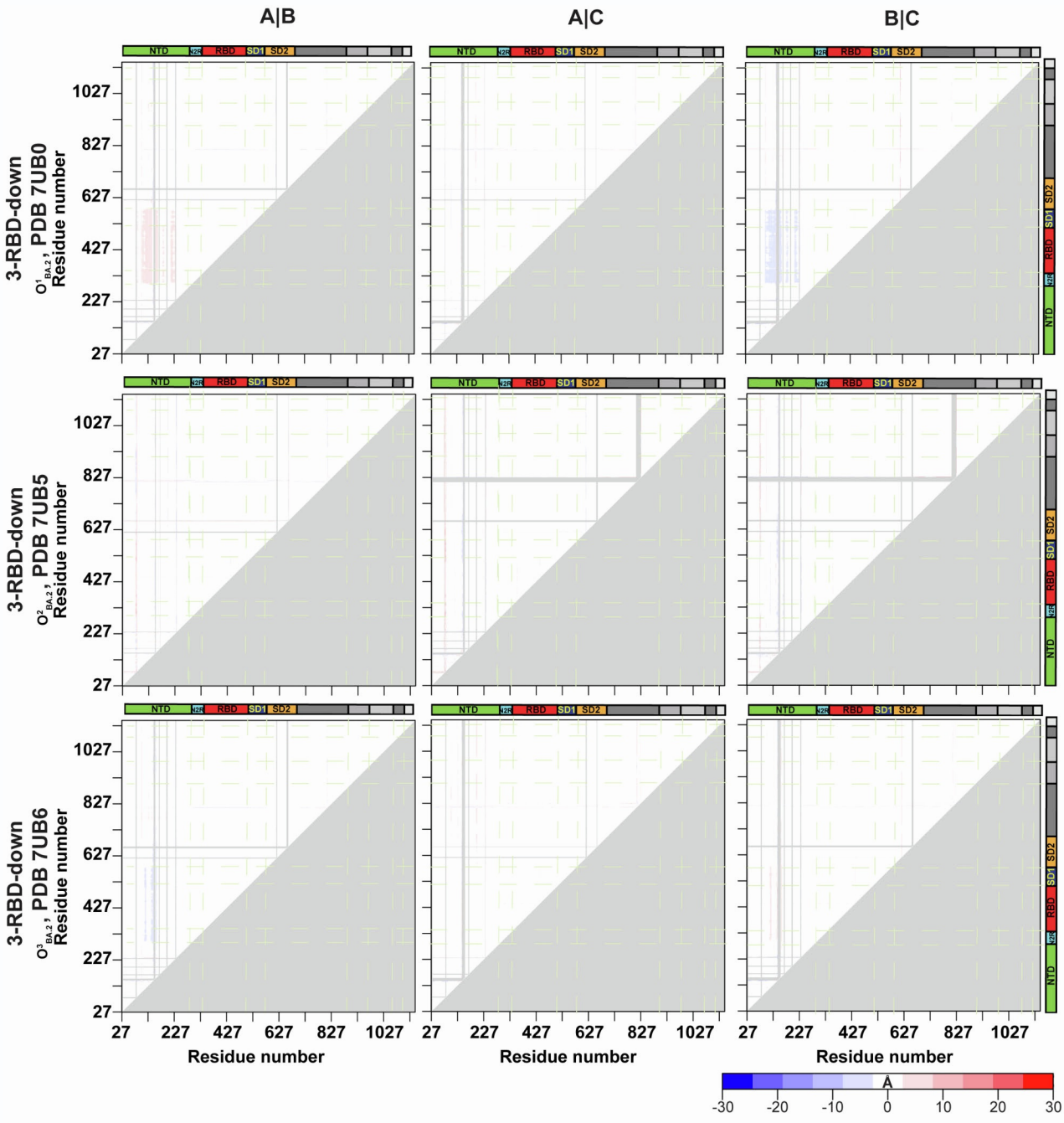

Data S3. Difference distance matrices (DDMs) analyses of S-GSAS-Omicron-BA.2 S ectodomain 3-RBD-down structures. Related to Figures 1 and 3, Table S1. Intrachain variability. Difference distance matrices (DDMs) provide superposition-free comparisons between a pair of structures by calculating the differences between the distances of each pair of Ca atoms in a structure and the corresponding pair of Ca atoms in the second structure. DDM of the 3-RBD down structures comparing each chain of a structure to the other chains of the same structure. The coloring scale used for the DDM analysis is represented on the bottom right corner.

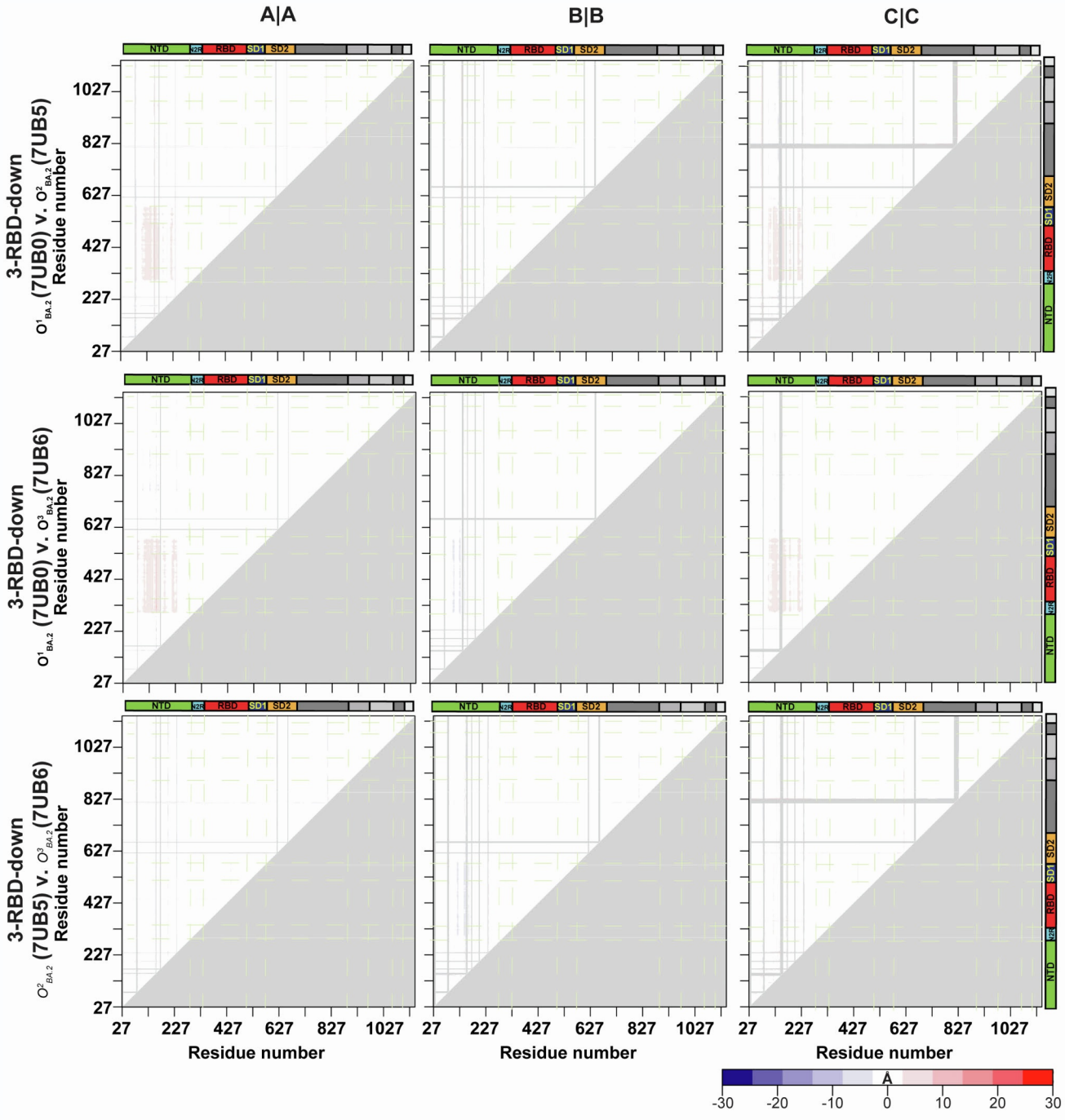

Data S3 continued. Difference distance matrices (DDMs) analyses of S-GSAS-Omicron-BA.2 S ectodomain 3-RBD-down structures. Related to Figures 1 and 3, Table S1. Interchain variability. DDM of the 3-RBD down structures comparing each chain of a structure to the same chain of another structure. The coloring scale used for the DDM analysis is represented on the bottom right corner.

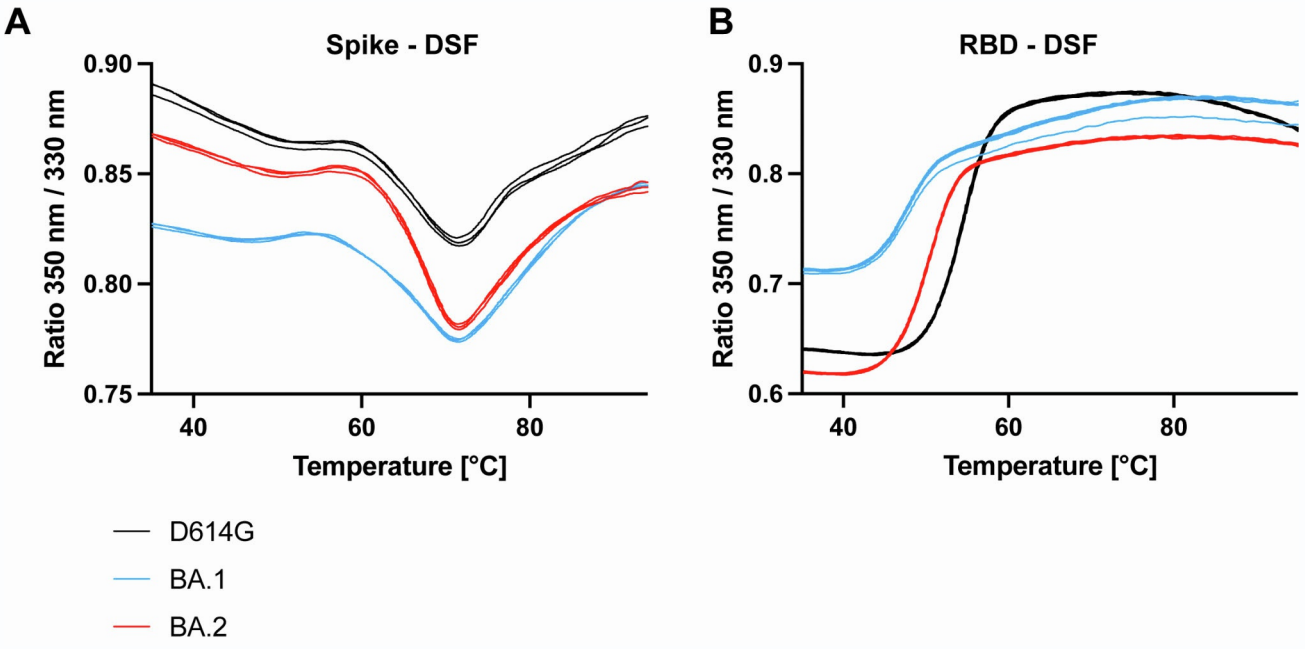

Data S4. Thermostability of SARS-CoV-2 S proteins and RBD proteins, Related to Figure 2. A. SARS-CoV-2 S protein DSF profiles showing changes in protein intrinsic fluorescence (expressed as a ratio between fluorescence at 350 and 330 nm). For each S protein construct (color coded as shown), three overlaid curves (technical replicates) are shown.

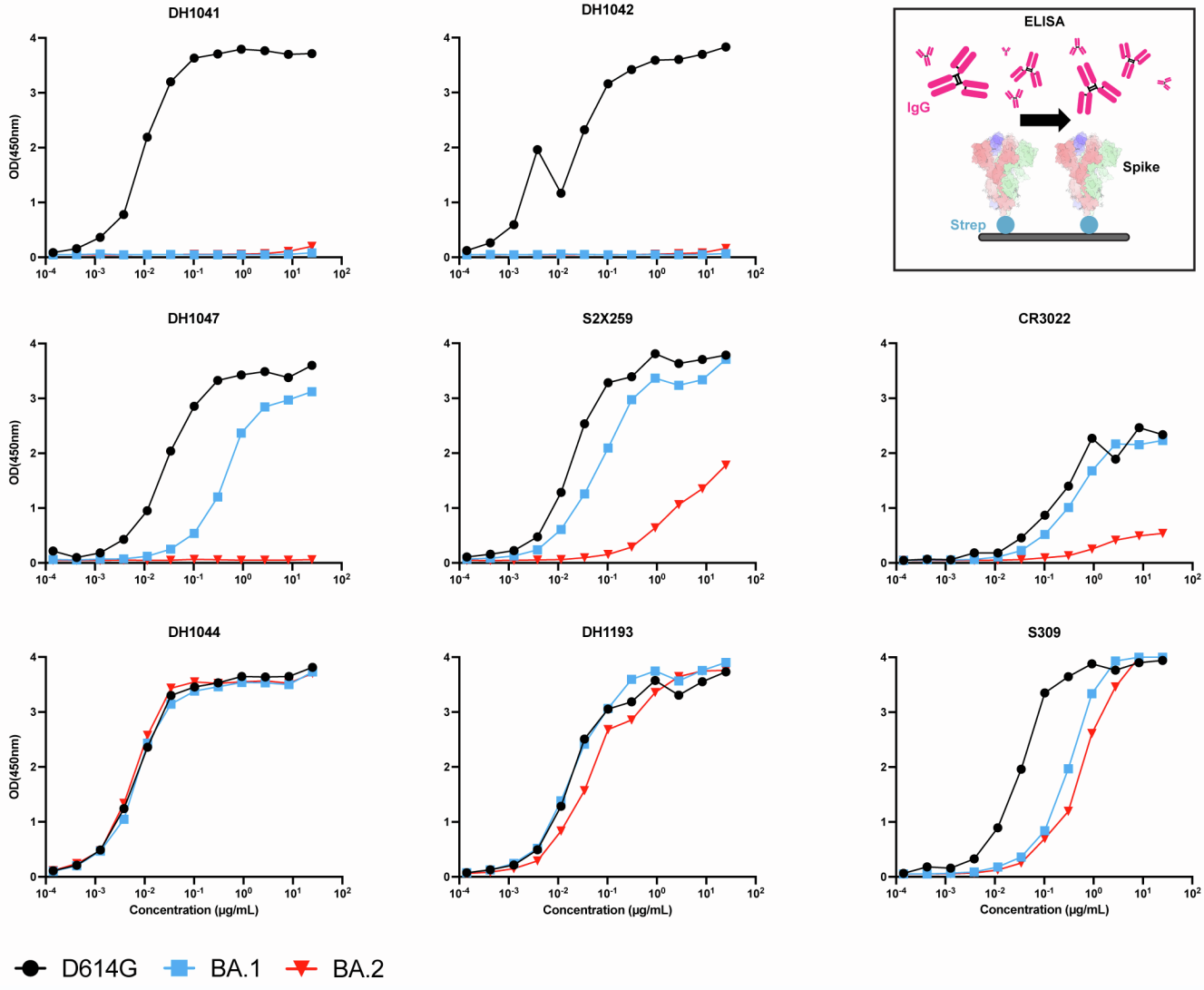

Data S5. Binding of RBD-directed antibodies to S protein and RBD variants, Related to Figures 5 and 6. ELISA binding of antibodies, top row, DH1041 and DH1042 (RBM-targeting), second row, DH1047, S2X259, and CR3022 (inner face RBD-targeting), and bottom row, DH1044, DH1193, and S309 (outer RBD face-targeting) to the D614G (black), BA.1 (blue) and BA.2 (red) S protein ectodomains. Schematic shows the assay format. Data are representative of at least two independent experiments.

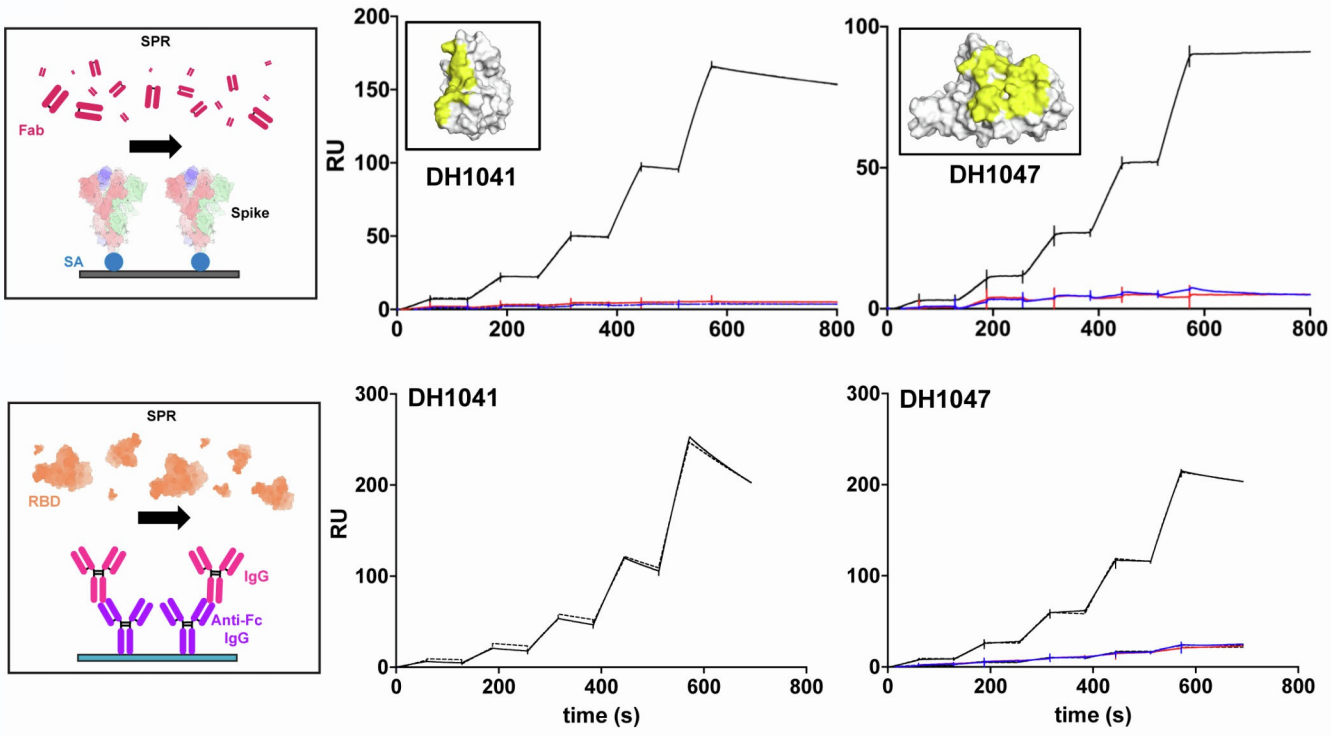

Data S5 continued. Binding of RBD-directed antibodies to S protein and RBD variants, Related to Figures 5 and 6. Binding of RBD-directed Fabs to S protein and RBD variants measured by SPR. **Top.** Schematic shows the assay format. Spike is captured on a Series S Streptavidin (SA) chip coated at 200 nM. Fabs were then injected at concentrations ranging from 0.5 nM to 8 nM, with a contact time of 60 seconds and a dissociation time of 120 seconds (50 µL/min) **Bottom.** Schematic shows the assay format. Antibodies were captured on a CM5 chip labeled with anti-Fc IgG antibodies. Binding of DH1044 and DH1193 Fabs to D614G (black), BA.1 (blue) and BA.2 (red) S protein ectodomains measured by SPR. The solid lines are the binding sensograms; the dotted lines show fits of the data to a 1:1 Langmuir binding model. Data shown are representative of at least two independent experiments.

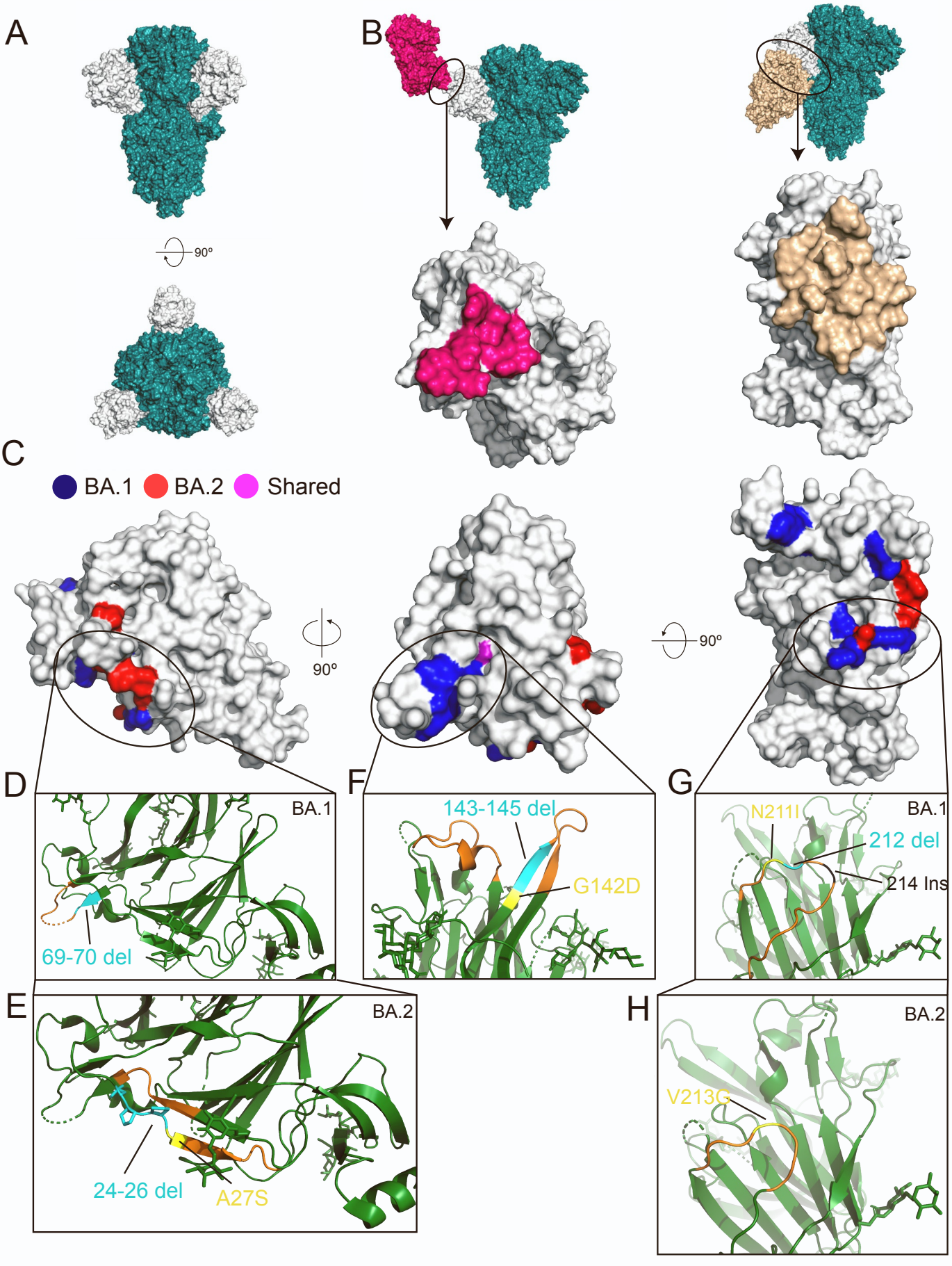
A
90°
B
C
BA.1
BA.2
Shared
90°
90°
D
BA.1
69-70 del
E
BA.2
24-26 del
A27S
F
143-145 del
G142D
G
N211I
BA.1
212 del
214 Ins
H
BA.2
V213G

Data S6. Comparison of N-terminal domain (NTD) mutations between BA.1 and BA.2 lineages. Related to Figure 5. **A.** Surface view of the spike trimer, teal, with each NTD shown in white, side view and top view. **B.** Surface views of the spike, with Fab regions of NTD-targeted antibodies bound: DH1050.1, pink, and DH1052, gold, are both shown and the NTD is shown in isolation, with residues contacted by the antibodies highlighted with the same color. Only one NTD is colored white and only one antibody Fab are shown in these views. **C.** Three views of the wild-type NTD with residues mutated in the Omicron variants highlighted as follows: blue: BA.1, red: BA.2, magenta: shared in BA.1 and BA.2. **D-H.** Cartoon and Stick views showing mutated residues from areas highlighted in C. Color scheme for d-h is as follows: yellow: mutated residue, cyan: deleted residues, black: insertion site, orange: nearby residues/loop residues, other NTD residues: green. Models used: A: 7LAB, B: 7LCN (DH1050.1) and 7LAB (DH1052): C-H: 7LY3

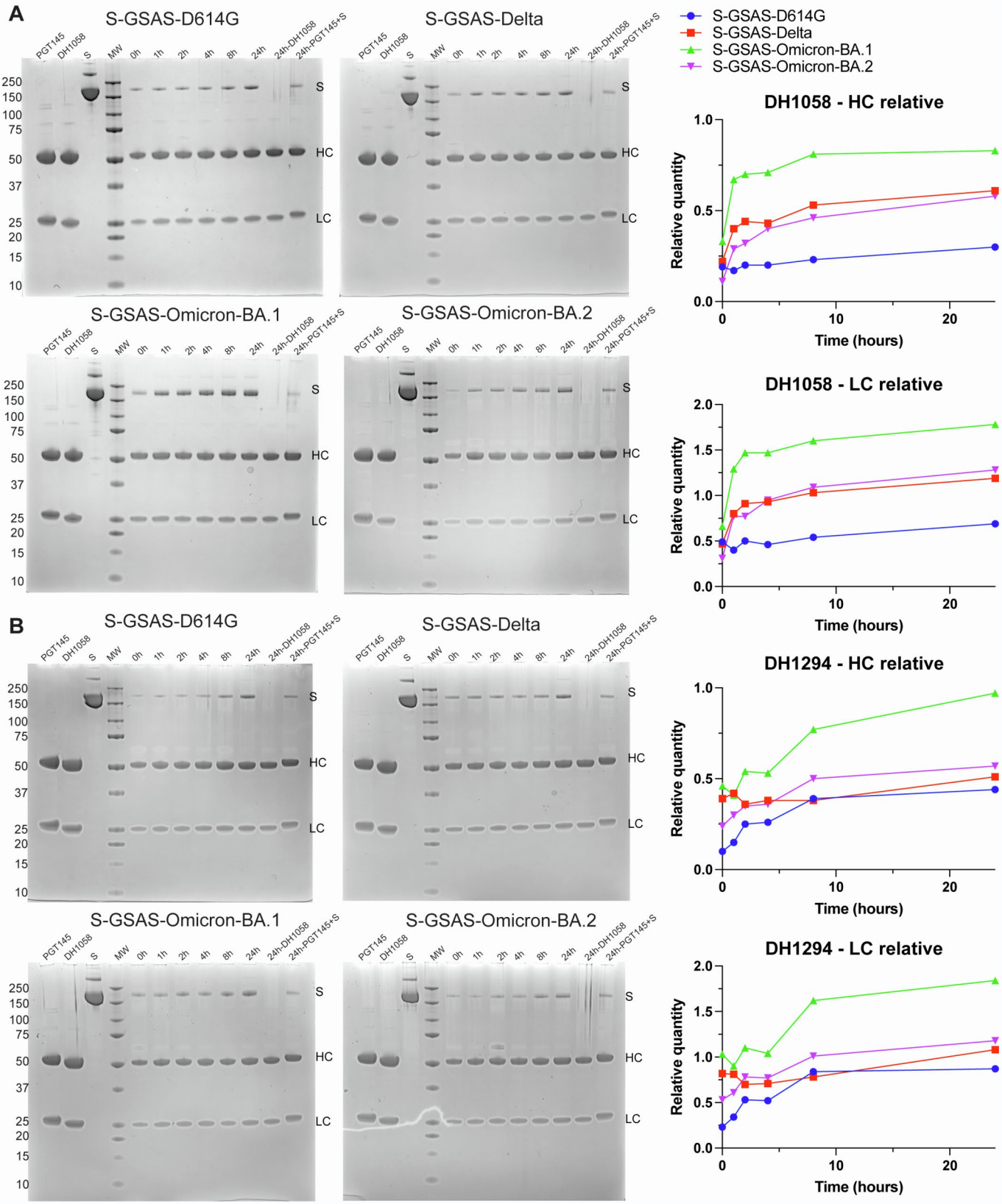
A
S-GSAS-D614G
S-GSAS-Delta
S-GSAS-Omicron-BA.1
S-GSAS-Omicron-BA.2
PGT145
DH1058
S
MW
0h
1h
2h
4h
8h
24h
24h-DH1058
24h-PGT145+S
250
150
100
75
50
37
25
20
15
10
S
HC
LC
S-GSAS-D614G
S-GSAS-Delta
S-GSAS-Omicron-BA.1
S-GSAS-Omicron-BA.2
DH1058 - HC relative
DH1058 - LC relative
DH1294 - HC relative
DH1294 - LC relative
Relative quantity
Time (hours)
0.0
0.5
1.0
1.5
2.0
0
10
20
B

Data S7. Time dependent exposure of fusion peptide (FP) to FP-directed antibodies, Related to Figure 7. A. Left. Reducing SDS-PAGE of immunoprecipitation of S-GSAS-D614G, S-GSAS-Delta, S-GSAS-Omicron-BA.1 and S-GSAS-Omicron-BA.2 using FP-directed antibody DH1058 bound to a Protein A coupled resin. Right. Intensity of the S protein band at each time point was normalized with the intensity of the heavy chain (HC, top) or light chain (LC, bottom) band. **B.** Same as **A.** but for antibody DH1294. Data shown are representative of at least two independent experiments.